

Synthesis, Structure, Spectroscopic Properties, and Photochemistry of Homo- and Heteropolynuclear Copper(I) Complexes Bridged by the 2,5-Bis(2-pyridyl)pyrazine Ligand

Taro Tsubomura,* Shinya Enoto, Shinya Endo, Tsuyoshi Tamane, Kenji Matsumoto, and Toshiaki Tsukuda

Department of Applied Chemistry, Seikei University, Kichijoji-kitamachi, Musashino, Tokyo 180-8633, Japan

Received January 21, 2005

Cu(I)–Cu(I) and Cu(I)–Ru(II) dinuclear complexes bridged by the 2,5-bppz (2,5-bis(2-pyridyl)pyrazine) ligand have been prepared and characterized including the X-ray crystallographic study of the dinuclear $[\{Cu(PPh_3)_2\}_2(\mu\text{-}2,5\text{-bppz})](PF_6)_2 \cdot 2CH_3Cl$ complex: $a = 13.974(2)$, $b = 13.993(2)$, $c = 13.537(2)$ Å; $\alpha = 101.98(1)$, $\beta = 103.22(1)$, $\gamma = 113.90(1)^\circ$; triclinic, $P\bar{1}$, $Z = 1$. The trinuclear $[\{(bpy)_2Ru^II(\mu\text{-}2,5\text{-bppz})\}_2Cu^I](PF_6)_5$ complex was also prepared, and the structure of the complex in solution was studied by spectrometric titration. The dinuclear Cu(I) complex and $[(bpy)_2Ru^II(\mu\text{-}2,5\text{-bppz})Cu^I(PPh_3)_2](PF_6)_5$ show photoluminescence in the solid state, which should arise from MLCT states. Photochemical oxidation of the trinuclear $Ru^II_2Cu^I$ complex occurs in the presence of oxygen to give a $Ru^II_2Cu^II$ complex. The MLCT states and the redox reaction in the excited state are discussed.

Introduction

2,5-Bis(2-pyridyl)pyrazine, 2,5-bppz, is known as a bridging ligand used to construct the dinuclear complexes¹ of copper(II), iron(II), and manganese(II) as well as the coordination polymers of copper(II)² and cadmium(II).³ The ligand has also been used to prepare supramolecular photoactive complexes of dinuclear to tetranuclear ruthenium complexes.^{4,5} The polynuclear ruthenium complexes have been shown to have rich electrochemical and photophysical properties.

Recently, photophysical and photochemical properties of copper(I) have increasingly attracted attention.⁶ Specially designed copper(I) complexes have long lifetimes for the excited MLCT state.⁷ Potential applications of these complexes for photovoltaic cells or electroluminescent displays

have been explored.⁸ Some polynuclear metal complexes containing copper(I) which are mainly designed for supramolecular photoactive systems have been proposed. Several reports on Ru(II)–Cu(I) supramolecular complexes have been reported.⁹ Although Ru(II)–Cu(I) complexes bridged by 2,3-bis(2-pyridyl)pyrazine (2,3-bppz) were reported,¹⁰ copper(I) complexes containing 2,5-bppz have not been published yet. As a part of our study on luminescent d¹⁰ metal complexes,¹¹ we have been examining the photophysical properties of Cu(I) complexes.¹² In this work, Cu(I)–Cu(I) homodinuclear and Cu(I)–Ru(II) heteromultinu-

* To whom correspondence should be addressed. E-mail: tsubomura@st.seikei.ac.jp.

(1) Neels, A.; Stoeckli-Evans, H. *Chimia* **1993**, *47*, 198.

(2) (a) Neels, A.; Stoeckli-Evans, H.; Escuer, A.; Vicente, R. *Inorg. Chem.* **1995**, *34*, 1946. (b) Neels, A.; Stoeckli-Evans, H.; Escuer, A.; Vicente, R. *Inorg. Chim. Acta* **1997**, *260*, 189.

(3) Neels, A.; Stoeckli-Evans, H. *Inorg. Chem.* **1999**, *38*, 6164.

(4) Ernst, S.; Kasack, V.; Kaim, W. *Inorg. Chem.* **1988**, *27*, 1146.

(5) Denti, G.; Campagna, S.; Sabatino, L.; Serroni, S.; Ciano, M.; Balzani, V. *Inorg. Chem.* **1990**, *29*, 4750.

(6) Kutal, C. *Coord. Chem. Rev.* **1990**, *99*, 213. McMillin, D. R.; McNett, K. M. *Chem. Rev.* **1998**, *98*, 1201. Armaroli, N. *Chem. Soc. Rev.* **2001**, *30*, 113.

(7) Cuttell, D. G.; Kuang, S.-M.; Fanwick, P. E.; McMillin, D. R.; Walton, R. A. *J. Am. Chem. Soc.* **2002**, *124*, 6. Kuang, S.-M.; Cuttell, D. G.; McMillin, D. R.; Fanwick, P. E.; Walton, R. A. *Inorg. Chem.* **2002**, *41*, 3313.

(8) Ma, Y.-G.; Chan, W.-H.; Zhou, X.-M.; Che, C.-M. *New J. Chem.* **1999**, 263. Sakaki, S.; Kuroki, T.; Hamada, T. *J. Chem. Soc., Dalton Trans.* **2002**, 840.

(9) Lam, M. H. W.; Cheung, S. T. C.; Fung, K.-M.; Wong, W.-T. *Inorg. Chem.* **1997**, *36*, 4618. Riklin, M.; Tran, D.; Bu, X.; Laverman, L. E.; Ford, P. C. *J. Chem. Soc., Dalton Trans.* **2001**, 1813. Grossshenny, V.; Ziessel, R. *J. Chem. Soc., Dalton Trans.* **1993**, 817. Ziessel, R.; Matt, D.; Toupet, L. *J. Chem. Soc., Chem. Commun.* **1995**, 2033.

(10) Scott, S. M.; Gordon, K. C.; Burrell, A. K. *J. Chem. Soc., Dalton Trans.* **1999**, 2669.

(11) Siddique, Z. A.; Ohno, T.; Nozaki, K.; Tsubomura, T. *Inorg. Chem.* **2004**, *43*, 663. Tsubomura, T.; Abe, M.; Tarutani, M.; Yamada, H.; Tsukuda, T. *Bull. Chem. Soc. Jpn.* **2003**, *76*, 2151.

(12) Tsubomura, T.; Takahashi, N.; Saito, K.; Tsukuda, T. *Chem. Lett.* **2004**, *33*, 678.

clear complexes bridged by the 2,5-bppz ligand were prepared for the first time, and their photophysical and photochemical properties have been studied.

Experimental Section

Material and Analytical Methods. $[\text{Cu}(\text{CH}_3\text{CN})_4]\text{PF}_6$ was prepared by a literature method.¹³ $[\text{Cu}(\text{PPh}_3)_4]\text{PF}_6$ was synthesized from $[\text{Cu}(\text{CH}_3\text{CN})_4]\text{PF}_6$ according to Rader's method.¹⁴ CHN percentages of the complexes were analyzed by a Perkin-Elmer 2400 instrument. The contents of copper were measured by an atomic absorption spectrometer, Shimadzu AA-6200, using the D₂ background correction mode.

2,5-bppz. The ligand was prepared by a modified method of Case et al.,¹⁵ as follows. To a solution of *O*-*p*-toluenesulfonyl-2-acetylpyridine oxime (10 g, 0.0345 mol, dissolved in 50 mL of dried ethanol) was added potassium *tert*-butoxide (5.4 g, 0.048 mol) gradually. The mixture was stirred vigorously, and potassium *p*-toluenesulfonate deposited was separated by filtration and washed with ether. The filtrate and the washings were combined, and a further 500 mL of ether was added to the mixture. The salt deposited was again separated by filtration, and the solid was washed with ether. The filtrate and washings were combined and concentrated to a small volume. The salt further deposited was separated by filtration, and a 30% aqueous solution of hydrogen peroxide (5 mL) was added to the filtrate. After the exothermal reaction was stopped, the mixture was kept in a refrigerator overnight. The yellow needles obtained were separated by filtration, washed with water followed by methanol, and dried in vacuo. Yield: 15%, 0.66 g. ¹H NMR (CD_3Cl): δ 9.4 (br, 2H), 8.70 (d, 2H), 8.40 (dd, 2H), 8.02 (dd, 2H), 7.50 (dd, 2H), 7.38–7.42 (m, 12H, *p*-Ph), 7.19–7.32 (m, 48H, *o*- and *m*-Ph).

$[\text{Ru}(\text{bpy})_2(2,5\text{-bppz})](\text{PF}_6)_2$ (1) was prepared by a literature method.⁶ Separation of the mononuclear complex from dinuclear complex is achieved by column chromatography over LH-20 gel using a methanol–acetonitrile mixed solvent as an eluent. Two singlets were found in the ¹H NMR (CD_3CN); δ 9.60 and 8.69 are characteristic of the protons on the pyrazine ring.¹⁶

$[\{\text{Cu}^{\text{I}}(\text{PPh}_3)_2\}_2(\mu\text{-}2,5\text{-bppz})](\text{PF}_6)_2$ (2). 2,5-bppz (0.1 mmol, 0.023 g) and $[\text{Cu}(\text{PPh}_3)_4]\text{PF}_6$ (0.2 mmol, 0.253 g) were successively dissolved in dichloromethane and stirred at room temperature under argon. After 90 min, red precipitates deposited were separated by filtration. The precipitates were dried in vacuo. Anal. Calcd for $[\{\text{Cu}(\text{PPh}_3)_2\}_2(\mu\text{-}2,5\text{-bppz})](\text{PF}_6)_2 \cdot 1/2\text{CH}_2\text{Cl}_2$, $\text{C}_{86.5}\text{H}_{71}\text{N}_4\text{Cu}_2\text{P}_6\text{F}_{12}\text{Cl}$: C, 59.60; H, 4.11; N, 3.21. Found: C, 59.31, H, 3.77; N, 3.49. ¹H NMR (CD_3CN): δ 9.4 (br, 2H), 8.70 (d, 2H), 8.40 (dd, 2H), 8.02 (dd, 2H), 7.50 (dd, 2H), 7.38–7.42 (m, 12H, *p*-Ph), 7.19–7.32 (m, 48H, *o*- and *m*-Ph).

$[\{\text{bpy}\}_2\text{Ru}^{\text{II}}(\mu\text{-}2,5\text{-bppz})_2\text{Cu}^{\text{I}}](\text{PF}_6)_5$ (3). To a solution of $[\text{Ru}(\text{bpy})_2(2,5\text{-bppz})](\text{PF}_6)_2$ (187 mg, 0.2 mmol) in dichloromethane was added $[\text{Cu}(\text{CH}_3\text{CN})_4]\text{PF}_6$ (75 mg, 0.2 mmol), and the new solution was stirred at room temperature under argon for 2 h. Concentration of the solution afforded black microcrystals (0.13 g, 60%), which were separated and washed with ether. Anal. Calcd for $[\{\text{bpy}\}_2\text{Ru}(2,5\text{-bppz})_2\text{Cu}](\text{PF}_6)_5 \cdot 4\text{H}_2\text{O}$, $\text{C}_{68}\text{H}_{60}\text{N}_{16}\text{O}_4\text{P}_5\text{F}_{30}\text{Ru}_2\text{Cu}$: C, 37.89; H, 2.81; N, 10.40; Cu, 2.95. Found: C, 37.99; H, 2.46; N, 10.33; Cu, 2.68.

(13) Kubas, G. J. *Inorg. Synth.* **1990**, 28, 68.

(14) Rader, R. A.; McMillin, D. R.; Buckner, M. T.; Matthews, T. G.; Casadonte, D. J.; Lengel, R. K.; Whittaker, S. B.; Darmon, L. M.; Lytle, F. E. *J. Am. Chem. Soc.* **1981**, 103, 5906.

(15) Case, F. H.; Koft, E. *J. Am. Chem. Soc.* **1958**, 81, 905.

(16) Campagna, S.; Denti, G.; De Rosa, G.; Sabatino, L.; Ciano, M.; Balzani, V. *Inorg. Chem.* **1989**, 28, 2565.

Table 1. Crystal Data and Experimental Details for the X-ray Analysis of $[\{\mu\text{-}2,5\text{-bppz}\}\text{Cu}^{\text{I}}_2(\text{PPh}_3)_4](\text{PF}_6)_2 \cdot 2\text{CH}_3\text{Cl}$

empirical formula, fw	$\text{C}_{88}\text{H}_{72}\text{Cl}_6\text{Cu}_2\text{F}_{12}\text{N}_4\text{P}$, 1939.2
cryst dimens/mm	$0.52 \times 0.20 \times 0.06$
cryst system	triclinic
lattice params <i>a</i> , <i>b</i> , <i>c</i> /Å	13.974(2), 13.993(2), 13.537(2)
lattice params α , β , γ /deg	101.98(1), 103.22(1), 113.90(1)
$V/\text{\AA}^3$	2218.0(6)
space group, Z value	$P\bar{1}$ (No. 2), 1
$D_{\text{calc}}/\text{g cm}^{-3}$	1.452
$\mu(\text{Mo K}\alpha)/\text{mm}^{-1}$	0.840
radiatn ($\lambda/\text{\AA}$)	Mo K α (0.710 69)
temp/ $^{\circ}\text{C}$	23.0
scan type, rate/deg min ⁻¹	ω -2 θ , 6.0 (in ω)
scan width/deg	$0.94 + 0.30 \tan \theta$
$2\theta_{\text{max}}/\text{deg}$	60.0
no. of unique reflcns measd	10 863
corrections	abs (transm factors: 0.951–0.817) decay (0.84% decline)
function minimized	$\Sigma w(F_o^2 - F_c^2)^2$
least-squares weights	$w = 1/[\sigma^2(F_o^2) + (0.0476P)^2]$, where $P = (F_o^2 + 2F_c^2)/3$
no. of reflcns used in LS ($2\theta < 50.00^{\circ}$)	7816
no. of variables	532
R, Rw2 (all data)	0.236, 0.172
R, Rw2 ($I > 2\sigma(I)$)	0.065, 0.126
goodness of fit indicator	0.95
max shift/error in final cycle	0.02
max and min peak in final diff map/ $\text{e}^{-}\text{\AA}^{-3}$	0.45, -0.45

$[\{\text{bpy}\}_2\text{Ru}^{\text{II}}(\mu\text{-}2,5\text{-bppz})_2\text{Cu}^{\text{I}}](\text{PF}_6)_6$ (4). $[\text{Ru}(\text{bpy})_2(2,5\text{-bppz})](\text{PF}_6)_2$ (0.15 mmol, 0.111 g) and $\text{CuCl}_2 \cdot 2\text{H}_2\text{O}$ (2.25 mmol, 0.4 g) were dissolved in 10 mL of water. The mixture was stirred for 2 h; then adding a saturated aqueous solution of NH_4PF_6 afforded dark red precipitates. The precipitates (0.14 g, 27%) were obtained by filtration, washed with water, and dried in vacuo. Anal. Calcd for $[\{\text{bpy}\}_2\text{Ru}(2,5\text{-bppz})_2\text{Cu}](\text{PF}_6)_6$, $\text{C}_{68}\text{H}_{52}\text{N}_{16}\text{P}_6\text{F}_{36}\text{Ru}_2\text{Cu}$: C, 36.65; H, 2.35; N, 10.06; Cu, 2.86. Found: C, 36.72; H, 2.42; N, 9.92; Cu, 3.03.

$[\{\text{bpy}\}_2\text{Ru}^{\text{II}}(\mu\text{-}2,5\text{-bppz})\text{Cu}^{\text{I}}(\text{PPh}_3)_2](\text{PF}_6)_3$ (5). $[\text{Cu}(\text{PPh}_3)_4]\text{PF}_6$ (0.2 mmol, 0.25 g) and $[\text{Ru}(\text{bpy})_2(2,5\text{-bppz})](\text{PF}_6)_2$ (0.2 mmol, 0.187 g) were dissolved in CH_2Cl_2 , and the new solution was stirred for 2 h under argon atmosphere. Concentration of the solution under reduced pressure and addition of ether afforded dark red precipitates. The precipitates (0.26 g, 78%) were separated by filtration and washed with ether. Anal. Calcd for $[\{\text{bpy}\}_2\text{Ru}(2,5\text{-bppz})\text{Cu}(\text{PPh}_3)_2](\text{PF}_6)_3$, $\text{C}_{70}\text{H}_{56}\text{N}_8\text{P}_3\text{F}_{18}\text{RuCu}$: C, 50.32; H, 3.38; N, 6.71. Found: C, 49.88; H, 3.06; N, 7.26.

X-ray Crystallography of 2. X-ray-quality crystals of the dinuclear complex $[\{\text{Cu}^{\text{I}}(\text{PPh}_3)_2\}_2(\mu\text{-}2,5\text{-bppz})](\text{PF}_6)_2 \cdot 2\text{CH}_3\text{Cl}$ were grown in an acetonitrile–chloroform mixed solvent. A red prismatic crystal was glued on a glass fiber and mounted on a Rigaku AFC5S diffractometer. The experimental details and the crystal data are listed in Table 1. The weak reflections ($I < 5.0\sigma(I)$) were rescanned, and the counts were accumulated to ensure good counting statistics. The intensities of three representative reflections were measured after every 150 reflections. Over the course of data collection, the standards decreased by 0.8%. A linear correction factor was applied to the data to account for the decay.

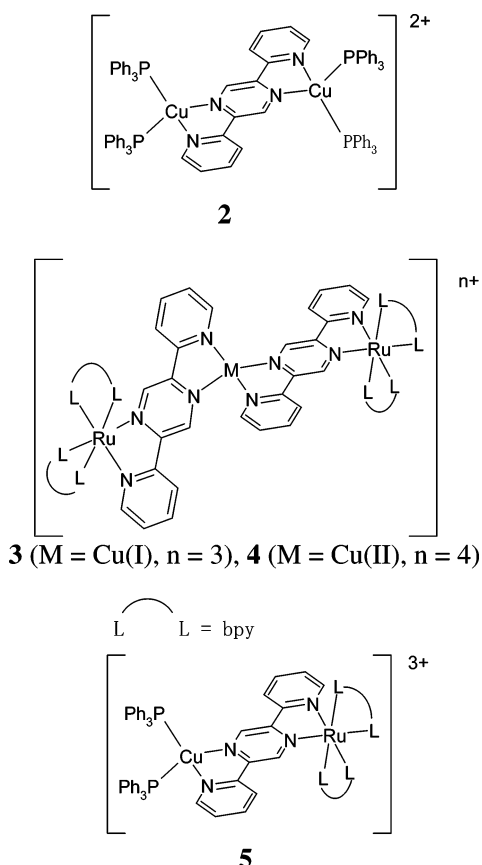
Calculations were performed using the *teXsan*¹⁷ crystallographic software package. The structure was solved by direct methods¹⁸ and expanded using Fourier techniques. SHELXL was used for

(17) *teXsan: Crystal Structure Analysis Package*; Molecular Structure Corp: The Woodlands, TX, 1985, 1999.

least-squares calculations.¹⁹ The non-hydrogen atoms were refined anisotropically. Hydrogen atoms were included but not refined.

Spectroscopic Measurements. Absorption and emission spectra were measured by Shimadzu UV-2100 and Shimadzu RF-5000 spectrometers equipped with R-955 (Hamamatsu) photomultiplier tube, respectively. All solution samples were degassed by freeze-pump-thaw cycles before the measurements. Emission spectra were studied using glass filters; one is a UV-pass filter (HOYA, U-330) to remove visible light in the excitation light, and one is a UV-cut filter (HOYA, UV-39) to avoid 2nd order diffraction. NMR spectra were recorded by a JEOL A-400 spectrometer using tetramethylsilane as a standard. Cyclic voltammograms were measured using a three-electrode method by a HUSO HECS 311B potentiostat and a HECS 321B potential sweeper. A platinum disk or glassy carbon disk electrode was used as the working electrode, and a platinum wire, as a counter electrode. An Ag/Ag⁺ reference electrode was used which was separated by a Vicor glass tip. The potential was calibrated using ferrocene as a standard ($E^\circ = 0.45$ V in CH₂Cl₂). The photochemical reaction is performed using a 250 W high-pressure mercury lamp equipped with a short-wavelength ($\lambda < 380$ nm) cut filter (HOYA L-38). The temperature was maintained at 20 °C during the photoirradiation using a thermostated water circulator.

Results and Discussion



Synthesis and Structure of the Dinuclear Copper(I) Complex.

The homodinuclear copper(I) complex, $[\{\text{Cu}^{\text{I}}$

(18) SIR92: Altomare, A.; Burla, M. C.; Camalli, M.; Cascarano, M.; Giovacazzo, C.; Guagliardi, A.; Polidori, G. *J. Appl. Crystallogr.* **1994**, 27, 435.

(19) SHELXL-97: Sheldrick, G. M. *Program for the Refinement of Crystal Structures*; University of Goettingen: Goettingen, Germany, 1997.

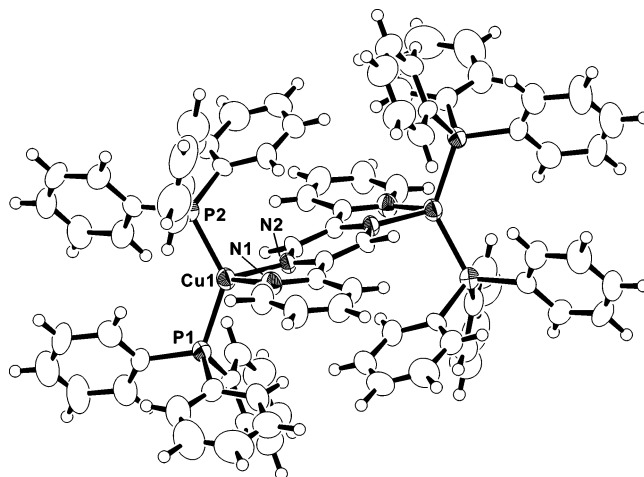


Figure 1. ORTEP drawing of the cation in **2**. Selected bond distances (Å) and angles (deg) are as follows: Cu1–P1, 2.260(3); Cu1–P2, 2.260(3); Cu1–N1, 2.090(8); Cu1–N2, 2.085(4); P1–Cu1–P2, 132.65(10); P1–Cu1–N1, 105.7(2); P1–Cu1–N2, 113.3(2); P2–Cu1–N1, 110.5(2); P2–Cu1–N2, 102.5(2); N1–Cu1–N2, 79.5(2).

$(\text{PPh}_3)_2\}_2(\mu\text{-}2,5\text{-bppz})](\text{PF}_6)_2$, **2**, was easily prepared from $[\text{Cu}(\text{PPh}_3)_4]^+$ and 2,5-bppz. Attempts to prepare a similar 2,5-bppz-bridged complex, $[\{\text{Cu}^{\text{I}}(\text{dppp})\}_2(\mu\text{-}2,5\text{-bppz})]^{2+}$ failed, where dppp = 1,3-bis(diphenylphosphino)propane. Crystals of $[\{\text{Cu}^{\text{I}}(\text{PPh}_3)_2\}_2(\mu\text{-}2,5\text{-bppz})](\text{PF}_6)_2 \cdot 2\text{CH}_3\text{Cl}$ were obtained by recrystallization using a chloroform–acetonitrile mixed solvent. The structure was solved by an X-ray crystallographic study, and a drawing of the cation is shown in Figure 1. A crystallographic inversion center is located at the center of the 2,5-bppz ligand. An asymmetric unit of the unit cell contains half of a dinuclear cation, one hexafluorophosphate anion, and a chloroform solvate molecule. The copper(I) has a distorted tetrahedral geometry. The P–Cu–P and N–Cu–N angles are 132.65(10) and 79.5(2)°, respectively, and the P–Cu–N angles are in the range 102.5–113.3°. The two Cu(I)–P distances are equal, and the two Cu(I)–N lengths also can be considered equal (see the caption of the figure). The bond length of the Cu–N(2,5-bppz) is longer than the reported length observed in the Cu(II) dinuclear 2,5-bppz complexes (2.00–2.04 Å),² but these lengths are in the normal range²⁰ for Cu(I) complexes. Crystal structures of some dinuclear and polynuclear metal complexes of the ligand 2,5-bppz have been studied by Neels et al. as described at the beginning of the paper. Examples are trinuclear zinc complexes, a polynuclear cadmium complex,³ dinuclear Ni(II) complexes,¹ and dinuclear Mn(II) and Fe(II) complexes.¹ In these papers, the conformation of coordinated 2,5-bppz has been discussed. The dihedral angles between the pyridine and pyrazine rings have been used as an index of the conformation and are in the range 3.9–16.2°. In this Cu(I) complex, the dihedral angle is 18.0(2)°, which is fairly large. Packing of the complex ions in the crystal lattice may be the cause of the staggered conformation. The closest intermolecular C–C distance is

(20) Miller, M. T.; Gantzel, P. K.; Karpishin, T. B. *Inorg. Chem.* **1999**, 38, 3414. Kirchoff, J. R.; McMillin, D. R.; Robinson, W. R.; Powell, D. R.; McKenzie, A. T.; Che, S. *Inorg. Chem.* **1985**, 24, 3928.

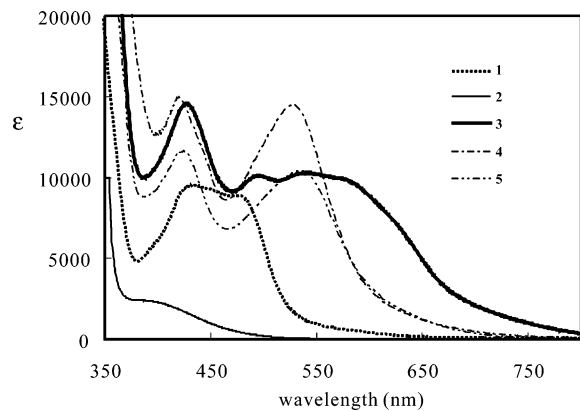


Figure 2. Absorption spectra of the complexes measured in dichloromethane solution at room temperature except for **2**, which was measured in acetonitrile.

3.59(2) Å between two phenyl groups of triphenylphosphine ligands, but no significant π stacking interaction is found in the lattice.

Some related structures of dinuclear copper(I) complexes have been reported. One is the 3,6-bis(2-pyridyl)-1,2,4,5-tetrazine (bptz) bridged dimer, $[(\mu\text{-bptz})\{\text{Cu}(\text{PPh}_3)_2\}_2]^{2+}$,²¹ and another one is the bipyrimidine (bpym) bridged complex, $[(\mu\text{-bpym})\{\text{Cu}(\text{PPh}_3)_2\}_2]^{2+}$.²² These reported structures show a considerable distortion from tetrahedral geometry around the copper ions compared to **2**. Both the bpym and bptz complexes include short π - π interactions between the bridging ligand and one of the phenyl groups of triphenylphosphine.

Absorption Spectra of 2. The absorption spectrum of **2** is shown in Figure 2. The spectrum shows a shoulder band at 380 nm with a molar extinction coefficient of $2500 \text{ M}^{-1} \text{ cm}^{-1}$. The Cu(I) to diimine MLCT bands of $[\text{Cu}(\text{diimine})\text{-}(\text{PPh}_3)_2]$ (diimine = phen or dmp) are known to exist at 365–370 nm with $\epsilon = 2500\text{--}3900 \text{ M}^{-1} \text{ cm}^{-1}$,²³ which are observed at shorter wavelength than the parent $[\text{Cu}(\text{diimine})]^{2+}$ complexes. Other mixed-ligand complexes, $[\text{Cu}(\text{dmp})(\text{diphosphines})]^+$, have been reported to show MLCT bands at 370–400 nm.⁷ The absorption band of the 2,5-bppz ligand itself was observed at 320 nm with $\epsilon = 3500 \text{ M}^{-1} \text{ cm}^{-1}$. The 380 nm band observed for **2** should be assigned to the Cu(I) to 2,5-bppz MLCT band. It should be noted that dissociation of a part of the phosphine ligands is possible in acetonitrile solution, but we cannot measure the spectrum of **2** in noncoordinating solvent such as dichloromethane due to the solubility problem.

Synthesis and Characterization of Ru–Cu Complexes.

The syntheses of the Ru–Cu–Ru and Ru–Cu complexes are straightforward. For example, the reaction of $[\text{Ru}(\text{bpy})_2\text{-}(2,5\text{-bppz})](\text{PF}_6)_2$ with $[\text{Cu}(\text{CH}_3\text{CN})_4]\text{PF}_6$ in dichloromethane affords black crystals of **3**. The analytical data (C, H, N, and Cu) for the product coincide with the calculated value of the trinuclear complex, $[\{(\text{bpy})_2\text{Ru}^{\text{II}}(\mu\text{-}2,5\text{-bppz})\}_2\text{Cu}^{\text{I}}\text{-}$

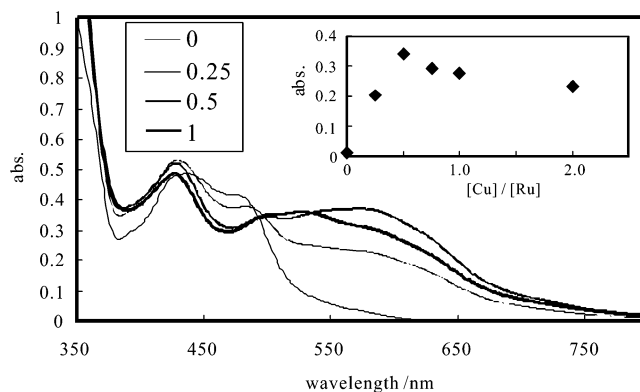


Figure 3. Change in the absorption spectra of solutions of **1** with increasing concentration of $[\text{Cu}(\text{CH}_3\text{CN})_4]^+$. Added molar ratios, $[\text{Cu}(\text{I})]/[\text{Ru}(\text{II})]$, are shown in the upper left inset. The change in the absorption intensities at 600 nm is shown in the right inset.

$(\text{PF}_6)_5$. **4** and **5** are similarly prepared. To confirm the nuclearity of the complexes, ESI mass and MALDI-TOF mass spectral analyses of **3–5** were tried, but they failed to detect the multinuclear complexes. Thus, changes in the absorption spectra of the solution containing $[\text{Ru}(\text{bpy})_2(2,5\text{-bppz})]^{2+}$ with addition of Cu(I) ion have been examined. As shown in Figure 2, the starting Ru(II) complex **1** shows low absorption intensity in the region $\lambda > 600 \text{ nm}$; however, **3** has very broad absorption bands which cover almost all the range of the visible region. Figure 3 shows the change in the absorption spectra recorded in a dichloromethane solution of **1** with increasing concentration of $[\text{Cu}(\text{CH}_3\text{CN})_4]^+$. The concentration of the ruthenium(II) complex was maintained at $5 \times 10^{-5} \text{ M}$. The change in the absorption spectra is not simple, but an absorption band emerged in the long-wavelength region when $[\text{Cu}(\text{CH}_3\text{CN})_4]^+$ was added to the solution. The maximum intensity at 600 nm is given at the $[\text{Cu}]/[\text{Ru}]$ ratio of 0.5, and the absorption gradually reduces when the ratio further increases from 0.5 to 2. The absorption spectrum at the ratio of 0.5 is close to that of the CH_2Cl_2 solution of isolated complex **3**. This result clearly shows that the complex **3**, which has an absorption band in the long-wavelength region, has a 2:1 molar ratio of Ru:Cu. It should be noted that the complex **3** may be a mixture of diastereomers due to chiral centers on Ru(II) and Cu(I). The absorption spectrum of **3** exhibits bands at 427, 496, and 533 nm with a shoulder at 580 nm. Since the molar absorption coefficient is similar to that of the MLCT bands of **1**, the bands would be assigned essentially to Ru(II) to 2,5-bppz MLCT transition. Coordination of Cu(I) to 2,5-bppz should cause the lowering of the π^* level of 2,5-bppz,¹⁰ which will be discussed later.

If the absorption spectrum of **3** was recorded in an acetonitrile solution, the spectrum is almost identical with that of the starting mononuclear ruthenium complex, **1**. The NMR spectrum of **3** in acetonitrile- d_3 also coincides with that of **1**. The observation shows that **3** decomposes into **1** and $[\text{Cu}(\text{CH}_3\text{CN})_4]^+$ in acetonitrile. We tried to measure the NMR spectrum of **3** in CD_2Cl_2 but failed due to the limited solubility in the solvent.

The absorption spectrum of **4** has two bands, at 420 and 528 nm, which are also assigned to MLCT bands involving

(21) Gordon, K. C.; Burrell, A. K.; Simpson, T. J.; Page, S. E.; Kelso, G.; Polson, M. I. J.; Flood, A. *Eur. J. Inorg. Chem.* **2002**, 554.
 (22) Vogler, C.; Hausen, H.-D.; Kaim, W.; Kohlmann, S.; Kramer, H. E. A.; Rieker, J. *Angew. Chem., Int. Ed. Engl.* **1989**, *28*, 1659.
 (23) Palmer, C. E. A.; McMillin, D. R. *Inorg. Chem.* **1987**, *26*, 3837.

the ruthenium(II) center. **5** has similar absorption bands at 425 and 535 nm.

The absorption spectrum of the $[\text{Ru}(\text{bpy})_2(2,3\text{-bppz})\text{Ru}(\text{bpy})_2]^{4+}$ dimer shows two discrete MLCT bands in the region 400–580 nm.⁵ In the dimeric complex, the bridging ligand becomes easier to reduce, and as a consequence, the Ru to 2,3-bppz CT band moves to lower energy. At the same time, the Ru to bpy CT band moves slightly to the blue.⁵ The two absorption bands shown for **4** and **5** may be discussed in a manner similar to that for the bands of the Ru_2 dimer. To confirm the origin of the red shift of the heteromultinuclear complexes, an electrochemical study was performed.²⁴ Cyclic voltammograms of **1** shows redox couples, $[\mathbf{1}]^{2+}/[\mathbf{1}]^{3+}$ and $[\mathbf{1}]^+ / [\mathbf{1}]^{2+}$, at $E_{1/2} = 1.50$ and -0.92 V, respectively, vs SCE in CH_2Cl_2 solution. The former corresponds to the oxidation of Ru(II)/Ru(III), and the latter, to formation of a 2,5-bppz anion radical.⁵ The CV of **5** shows an irreversible cathodic peak at -0.57 V when scanned at the range from -1.3 to $+0.3$ V.²⁵ We assigned the cathodic peak to the reduction of the 2,5-bppz ligand. This result means the lowering of the π^* level of the 2,5-bppz ligand by ca. 0.4 V, which should be the course of the red-shift of the MLCT band of **5** compared with that of **1**. The shift of the redox potential of the bridging ligand is larger than that of $[\text{Ru}(\text{bpy})_2(2,3\text{-bppz})\text{Cu}(\text{PPh}_3)_2]^{3+}$ reported by Scott et al.¹⁰ but smaller than that of $[\text{Ru}(\text{bpy})_2(2,5\text{-bppz})\text{Ru}(\text{bpy})_2]^{4+}$.⁵

The CV of **3** shows reduction peaks similar to that of **5**. There is an irreversible cathodic peak at -0.60 V (SCE) in addition to the peak at -0.98 V, which is a part of the quasi-reversible peaks at $E_{1/2} = -0.92$ V, when scanned at the range from -1.3 to $+1.7$ V. The cathodic -0.6 and -0.98 V peaks seem to correspond to the reduction of the 2,5-bppz and bpy ligands of **3**, respectively, and the former also shows the lowering of the π^* level of the 2,5-bppz ligand by ca. 0.4 V. The result illustrates that the π^* level of the bridging ligand in the trinuclear complex **3** is similar to that of **5**. Thus, the origin of the broad and further low-energy band shown in the trinuclear complex **3** is unclear; a possibility is further lowering of the $\pi-\pi^*$ level due to the interligand interaction of two 2,5-bppz ligands in the trinuclear complex.

Luminescence Spectra of the Complexes. The luminescence spectra of solid samples of the complexes are shown in Figure 4. Complexes **3** and **4** are not luminescent in the solid state or in solution. The binuclear Cu(I) complex **2** has an emission maximum at 700 nm (data not corrected for intensity) in the solid state. The $\pi-\pi$ interactions between the bridging ligand and one of the phenyl groups of triphenylphosphine were reported to be “prerequisites for the solid-state luminescence” of the bpm dinuclear complex,²² but **2** has no apparent $\pi-\pi$ interactions. A considerable red shift is observed compared with that of $[\text{Cu}(\text{phen})(\text{PPh}_3)_2]\text{-PF}_6$, the emission maximum of which was reported to 600 nm in methanol. The decay of the luminescence can be

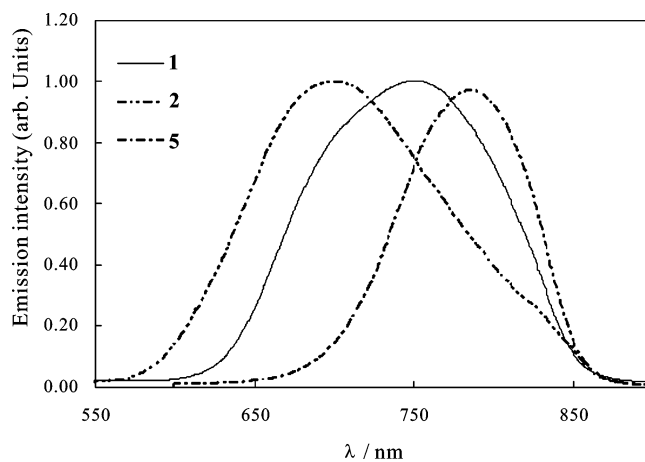


Figure 4. Uncorrected photoluminescence of the solid-state samples of the complexes **1**, **2**, and **5** measured at room temperature.

described as a single exponential with a lifetime of 320 ± 20 ns. The luminescent excited state of **2** should be ascribed to the MLCT state. The multiplicity of the luminescent states of the Cu(I) complexes has been extensively discussed. A recent report²⁶ reconfirms McMillin's assignment²³ that the dominant part of the luminescence occurs from a singlet MLCT state. **2** does not luminesce in acetonitrile solution, where an exciplex quenching²⁷ should occur.

Luminescence of **5** is observed in the solid state, although **5** is not luminescent in dichloromethane solution. The spectrum is illustrated in Figure 4, which also shows that of the starting complex, **1**. The lowest energy MLCT absorption of **5** is red-shifted by 50 nm compared to **1**. The red-shift of **5** from **1** observed in the luminescence spectra corresponds to that of the absorption shift, although the exact shift cannot be estimated from the figure because of the low sensitivity of the detector. Both of the decay profiles of the luminescence of **1** and **5** are not single exponential. The curves can be fitted with biexponential functions with $t = 50$ and 257 ns for **1** and 41 and 160 ns for **5**. The decay data are shown in the Supporting Information. The luminescence should arise from the $\text{Ru} \rightarrow 2,5\text{-bppz}^3$ MLCT state. The lowering of the π^* level of 2,5-bppz due to the coordination of Cu(I) may be the cause of the red-shift. The shorter lifetime of **5** in comparison to that of **1** can be explained by the energy-gap law or quenching by the copper(I) center.

Photooxidation of the Complex. We found that visible-light irradiation of **3** in CH_2Cl_2 causes a change in the absorption spectra of the complex. As shown in Figure 5, the absorption spectra of the photoproduct of the reaction almost agree with that of **4**. We have confirmed that the photochemical reaction does not proceed under argon atmosphere, and the reaction does not occur in the dark irrespective of the atmosphere. Thus, we conclude that **3** is photochemically oxidized to **4** using atmospheric oxygen as an oxidant.

The cyclic voltammogram of **3** recorded in CH_2Cl_2 solution shows an broad anodic peak at 1.1 V, in addition to the

(24) See Supporting Information. The cyclic voltammograms were recorded in dichloromethane solutions. The voltammogram of **4** cannot be measured because of the low solubility in the solvent.

(25) When the CV of **5** was recorded in the range from -1.3 to $+1.5$ V, irreversible changes of the entire voltammogram had occurred. Obviously, decomposition of the oxidation product of **5** occurred.

(26) Siddique, Z. A.; Yamamoto, Y.; Ohno, T.; Nozaki, K. *Inorg. Chem.* **2003**, *42*, 6366.

(27) Stacy, E. M.; McMillin, D. R. *Inorg. Chem.* **1990**, *29*, 393.

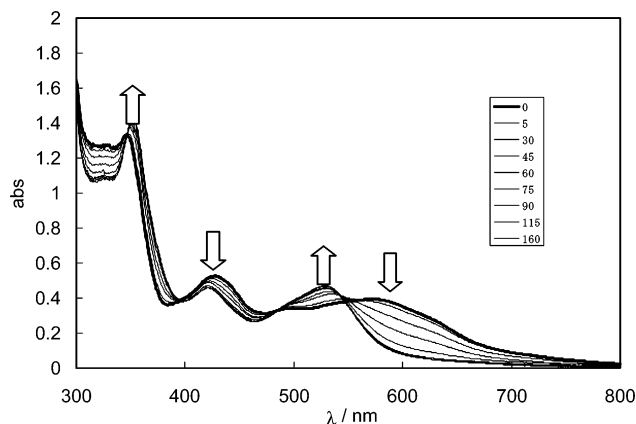


Figure 5. Change in the absorption spectra of **3** with irradiation of light. The duration times after starting the photoirradiation are shown in the small inset (minutes).

reversible couples of Ru(II)/Ru(III).²⁸ The value of the potential and the irreversible nature of the peaks should show that an irreversible Cu(I)/Cu(II) redox reaction occurs. The reduction potential in the excited state can be estimated from the ground-state oxidation potential of the Ru(II)–Cu(I) complex (1.1 V) and the energy of the excited state. The latter can be calculated to be 1.6 V from the energy of the lowest energy absorption band (ca. 600 nm).²⁹ Thus, the redox potential of Cu(I)/Cu(II) in the excited state of the multinuclear complex is as low as -0.5 V, which can be compared with the potential of $+1.1$ V in the ground state. This implies that the Ru(II)–Cu(I)–Ru(II) complex can be oxidized much more easily in the excited state than in the ground state. The fact that the photochemical reaction did

(28) See Supporting Information.

(29) Roundhill, D. M. *Photochemistry and Photophysics of Metal Complexes*; Plenum Press: New York, 1994.

not occur in the absence of air shows that dioxygen acts as an oxidant.

Conclusion

This work shows the copper(I) containing homo- and heteromultinuclear complexes can be prepared using the 2,5-bppz ligand for the first time. The homodinuclear copper complex **2** was structurally characterized by X-ray methods. The heterotrinnuclear Ru(II)–Cu(I)–Ru(II) complex **3** and two other complexes were prepared. The 2:1 metal ratio of **3** was retained in solution, which was confirmed by the spectrometric titration. Some complexes investigated do show photoluminescence due to MLCT excited states based on Cu(I)–2,5-bppz or Ru(II)–2,5-bppz. We also showed that photochemical oxidation of the heteromultinuclear complex occurs; the change in the absorption spectra of the solution of the complex is fairly clean. The lowering of the redox potential of Cu(I)/Cu(II) in the excited state should be the reason why photoirradiation promotes the oxidation reaction. The photochemistry of Cu(I) is of current interest in view of the interaction with DNA. The photoredox properties of multinuclear Cu(I) complexes will be further adjusted by designing a “complex ligand” that contain various kinds of bridging ligands and metal centers.

Acknowledgment. This work was supported by the Ministry of Education, Culture, Sports, Science, and Technology (Grant-in-Aid for Scientific Research) and by the Asahi Glass Foundation.

Supporting Information Available: A CIF file for complex **2**, cyclic voltammograms of complexes **1**, **3**, and **5**, and luminescence-decay curves of the solid-state samples. This material is available free of charge via Internet at <http://pubs.acs.org>.

IC0500980